Materials Physics and Mechanics 21 (2014) 112-118 Received: June 25, 2014

LIGHT EMISSION FROM CdHgTe–BASED NANOSTRUCTURES

K.D. Mynbaev[1,2*], A.V. Shilyaev[1], N.L. Bazhenov[1], A.I. Izhnin[3], I.I. Izhnin[3,4], A.V. Voitsekhovskii[4], N.N. Mikhailov[5], V.S. Varavin[5], S.A. Dvoretsky[4,5]

[1]Ioffe Institute, Polytechnicheskaya 26, Saint-Petersburg, 194021, Russia

[2]ITMO University, Kronverkskiy 49, Saint-Petersburg, 197101, Russia

[3]R&D Institute for Materials SRC "Carat", Stryjska 202, Lviv, 79031, Ukraine

[4]Tomsk State University, Lenina 36, Tomsk, 634050, Russia

[5]A.V. Rzhanov Institute of Semiconductor Physics, Siberian Branch of RAS, ac. Lavrentieva 13, Novosibirsk, 630090, Russia

*e-mail: mynkad@mail.ioffe.ru

Abstract. Optically excited light emission from CdHgTe nanostructures with 12 to 1100 nm–wide potential wells was studied. The structures were grown by molecular beam epitaxy on GaAs substrates. For structures with size quantization, radiative transitions between the levels of the electrons and light holes were observed. For structures with broad potential wells, optical transitions related to exciton localized at potential fluctuations were recorded. In the latter case, the significant degree of the alloy disorder led to the broadening of photoluminescence (PL) spectra and a considerable Stokes shift that could be traced up to temperature T~230 K. Annealing of the structures improved the ordering and led to the increase in the PL intensity. A remarkable feature of the PL of the structures was rather small decrease of its intensity with temperature increasing from 84 to 300 K. This effect was explained by localization of carriers at potential fluctuations.

1. Introduction

CdHgTe solid solutions, which for many years have served as basic materials for infrared photodetectors, recently emerged as materials for light emitters [1, 2]. A reason for that is the demand for optoelectronic devices for gas detection systems operating in the wavelength range 2–6 μm, where many gases have strong optical absorption. Similar to other modern semiconductor devices, CdHgTe light emitters are supposed to employ epitaxial nanostructures, and can be based both on quantum–well structures [3–5] and structures with a resonant cavity. The latter represent nanostructures with wide potential wells and with mirrors deposited at the both sides of spacer layers [2, 6, 7]. As a rule, optical pumping is used to excite emission from such structures [2, 7]. So far, CdHgTe–based emitters have been fabricated using epitaxial structures grown on 'native' Cd(Zn)Te substrates. These substrates provide excellent lattice and thermal expansion coefficient match, but are very expensive, limited in size and have low mechanical strength. Because of these drawbacks of Cd(Zn)Te, 'foreign' substrate technology using materials such as Si, Ge, and GaAs has been developed for CdHgTe–based photodetectors [8]. Despite the advancement of this technology, the emissive properties of CdHgTe nanostructures grown on 'foreign' substrates were not studied in detail yet. In this paper, we report on the results of the study of light emission from optically excited CdHgTe–based nanostructures grown on (013)GaAs.

© 2014, Institute of Problems of Mechanical Engineering

2. Experimental details

The nanostructures were grown with ZnTe/CdTe buffer layers at A.V. Rzhanov Institute of Semiconductor Physics (Novosibirsk, Russia). The details of the growth procedure can be found elsewhere [9]. The growth cycle was controlled by means of an automatic ellipsometer. The values of the solid solution composition were determined with *in situ* ellipsometric measurements and checked using *ex situ* optical transmission and photoconductivity studies. To relate the energy gap E_g to solid solution composition x, the $E_g(x,T)$ dependence from Ref. [10] was used. Parameters of the typical structures are listed in Table 1.

Table 1. Parameters of some of the nanostructures studied.

#	1	2	3	4	5	7	8	9	10	11
d_w, *nm*	200	200	200	100	50	200	400	1100	200	200
x	0.23	0.40	0.32	0.32	0.34	0.45	0.34	0.34	0.36	0.41
y	0.55	0.75	0.69	0.68	0.69	0.63	0.71	0.72	0.72	0.72

In typical nanostructures (#1 to #9), a $Cd_xHg_{1-x}Te$ potential well (x = 0.27–0.45) with the width d_w=50–1100 nm was sandwiched between two $Cd_yHg_{1-y}Te$ (y = 0.55–0.75) spacer layers with the thickness d_b=350–1000 nm. In structures ##10 and 11, a set of barrier layers with x~0.9 was added at the both sides of the spacers. To test the effect of spacer layer doping and post–growth treatment on optical properties of the structures, in structure #11 the spacers were *in situ* doped with In (donor) with concentration $\approx 3\times10^{15}$ cm^{-3}, and a number of structures was annealed in helium atmosphere (~250 °C, ~3 hours).

Light emission (photoluminescence, PL) was studied using a grating monochromator. The signal was excited by a semiconductor diode laser. The measurements were performed in a temperature range T=4.2–300 K. For signal detection, a cooled Ge:Au or InSb photodetector was used. For photoconductivity (PC) measurements, a similar set-up was used with a globar serving as a light source.

3. Results and discussion

3.1. Low-temperature photoluminescence. Upon studying the PL of nanostructures with various potential well widths, it was found that in relation to optical properties, samples with $d_w \leq 33$ (not listed in Table 1) were indeed “quantum–well” (QW) structures. Here, the main PL peak at low temperatures ($4.2<T<100$ K) was due to carrier recombination between QW levels, and the energy of an emitted photon was determined by the effective (with the energies of the levels taken into account) energy gap. The optical properties of these nanostructures will be discussed briefly in Section 3.3. The PL spectra of nanostructures with “broad” ($d_w \geq 50$ nm) potential wells (BPW) at low temperatures were dominated by the peak caused by recombination of an exciton localized in density–of–states tails. The energy of this peak E_{PL} was substantially lower than the energy gap E_g as calculated according to the values of x deduced from the ellipsometry data and optical transmission and photoconductivity measurements. At 4.2 K, the PL spectra of most of the as–grown BPW nanostructures represented a single Gaussian–shaped band with the full–width at half–maximum (FWHM) of 8 to 17 meV. As the temperature increased, delocalization occurred, and eventually $E_{PL}(T)$ followed $E_g(T)$. An example of such behavior is given in Fig. 1, which shows the temperature dependence of E_{PL} for a nanostructure with d_w=1000 nm, x=0.36 and y=0.54 (symbols) and calculated E_g (solid line). The magnitude of the deviation of $E_{PL}(T)$ from $E_g(T)$ (the Stokes shift) and the FWHM of the excitonic line at low temperatures reflect a degree of the solid solution (alloy) disorder [11]. As the observed FWHMs of 8 to 17 meV and the Stokes shifts (15 to 25 meV) greatly exceeded those calculated using disorder models [12] (5 to 6 meV,

depending on the composition) and experimentally observed in samples grown by, e.g., liquid–phase epitaxy [13], it was concluded that all the MBE–grown CdHgTe nanostructures, in addition to purely stochastic compositional fluctuations (which are typical of any semiconductor alloy), possessed a considerable degree of technology–induced disorder.

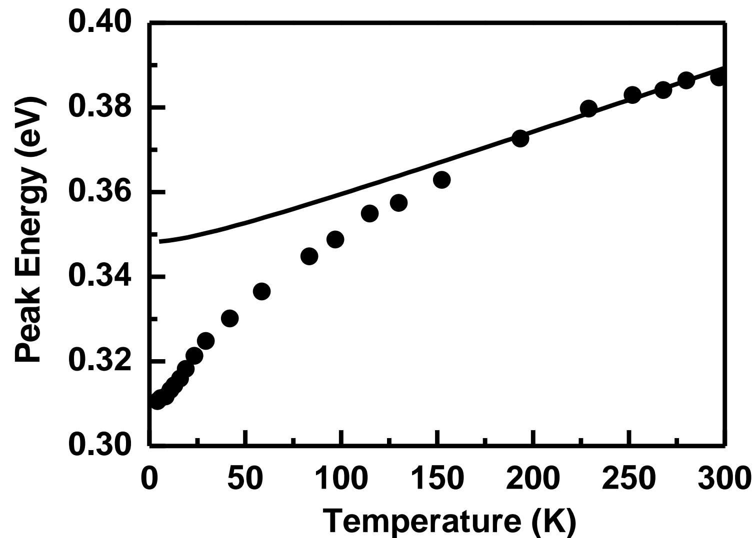

Fig. 1. Temperature dependence of the PL peak position for a BPW CdHgTe nanostructure (symbols). Solid line represents $E_g(T)$ calculated using Ref. [10] for CdHgTe with x=0.36.

Some of the structures demonstrated more complicated low-temperature PL spectra, which comprised a number of luminescence bands. An example is given in Fig. 2, which shows the PL spectra of as–grown structures ##9, 10 and 7, as recorded at T=84 K. Here, thin lines suggest deconvolution of the spectra of structure #10. For this structure, the low-energy line, presumably acceptor–related, was separated from the high–energy (excitonic) line by ~30 meV. For structure #4, a similar acceptor–related PL line was observed at 4.2 K (not shown). These relatively deep acceptor levels are different from shallow vacancy–related acceptor levels with the energy of ~14 meV, and can be attributed to defects specific to CdHgTe grown on GaAs [14].

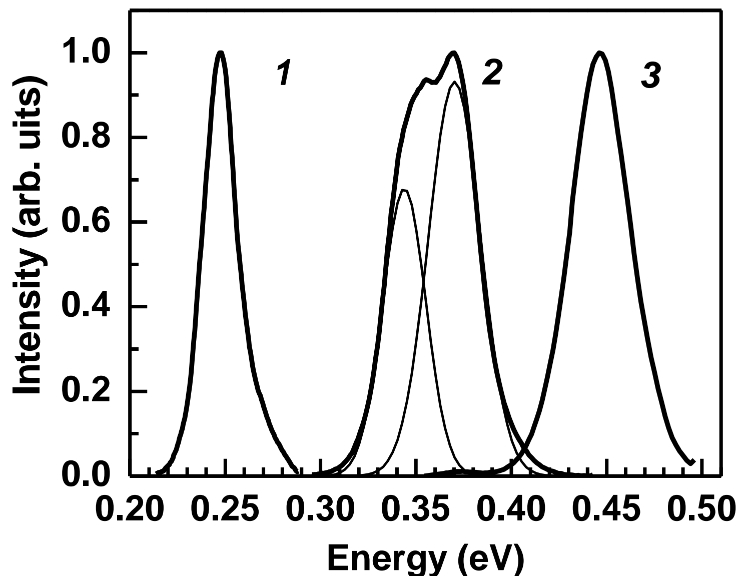

Fig. 2. PL spectra of BPW nanostructures ##9 (*1*), 10 (*2*) and 7 (*3*) recorded at T=84 K.

The FWHM of the excitonic lines at 84 K varied from 18 to 33 meV and did not depend on x, thus being determined solely by the degree of alloy disorder in each individual sample. These values were comparable to FWHMs of PL spectra of CdHgTe films grown by metal–organic vapor phase deposition, which were tested under similar conditions, and seemed to be typical of the material fabricated by methods that implemented non–equilibrium growth conditions. A number of films grown by liquid–phase epitaxy with composition varying from 0.29 to 0.39, when studied under similar conditions, yielded FWHM of the spectra of 16 to 20 meV, indicating much better alloy ordering.

3.2. High-temperature photoluminescence. All the studied structures demonstrated PL signal at room temperature with spectra having quite irregular shape, which indicated that they actually contained a number of separate emission bands. It is of interest that for many structures the intensity of the PL signal decreased with temperature increasing from 84 to 290 K not as strongly as was expected. An example of such phenomenon is given in Fig. 3.

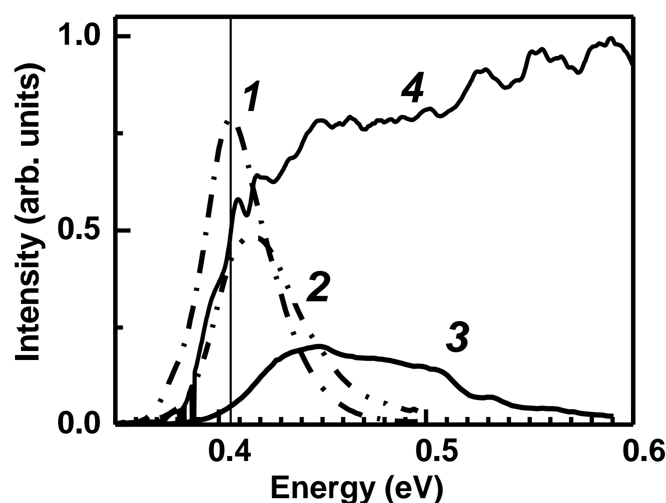

Fig. 3. PL spectra of BPW structure #2 recorded at 84 K (*1*), 137 K (*2*) and 300 K (*3*), and photoconductivity spectrum recorded at 84 K (*4*). Thin vertical line corresponds to the maximum of the 84 K PL peak, which coincides with the half–maximum of the PC signal at the same temperature.

As can be seen, with the temperature increasing, the PL intensity for structure #2 decreased only threefold. A similar effect was observed for other structures, with the PL intensity dropping from 20 % to fourfold while heating the samples from 84 to 290 K. Such a phenomenon was not expected for the narrow-gap CdHgTe, where Auger recombination is believed to be dominating at high temperatures. For example, in Fig. 4 the results of calculations are given representing carrier lifetime limited by radiative and Auger recombination in CdHgTe with x=0.30. Calculations were performed using a microscopic approach with taking into account non–parabolicity of the energy bands in narrow–gap CdHgTe, as described by Kane's theory, and considering the temperature dependence of the overlap integrals [15]. For p–type material, typical parameters of CdHgTe were used with acceptor concentration N_a=10^{15} cm^{-3} and acceptor level depth E_a=6 meV. For n–type material, donor concentration N_d=10^{15} cm^{-3} and donor level E_d=0 meV were assumed (in fact, all the studied as–grown nanostructures were of n–type with N_d–N_a=(0.5–2.0)×10^{15} cm^{-3}). The details of the calculations will be presented elsewhere. As can be seen in Fig. 4, at low temperatures the radiative lifetimes are indeed smaller than Auger ones, which means the dominance of radiative recombination and favors the observation of PL. Starting from ~230 K, however, calculations predict that Auger recombination dominates over radiative

one. Considering the fact that in real structures the interband Auger recombination is complemented with other types of recombination, such as Shockley-Read recombination, strong PL from narrow-gap CdHgTe (which we observed in nanostructures with composition down to x=0.29) at the room temperature does come as a surprise.

Regarding the shape of the spectra, as followed from the comparison of the PL and photoconductivity spectra, at room temperature the PL line which corresponded to E_g, was always the line with the lowest energy (compare to photoconductivity spectrum at 84 K in Fig. 3). The high–energy lines corresponding to emission of photons with energy greater than E_g started to show in the spectra at a certain temperature in the 120–290 K range.

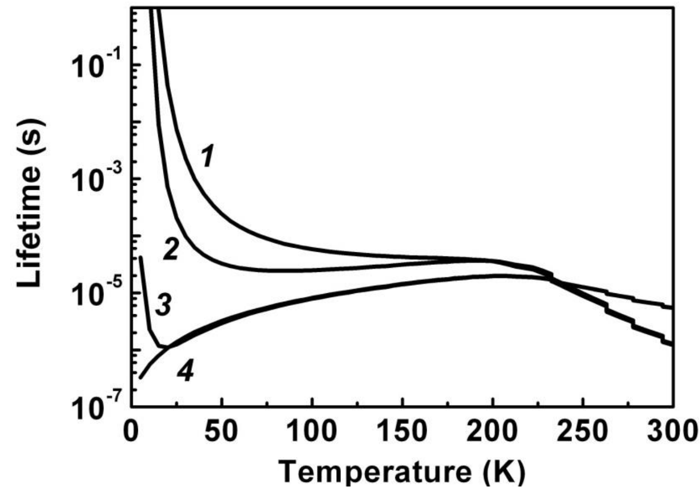

Fig. 4. Calculated Auger (*1,2*) and radiative (*3,4*) recombination–limited lifetimes in CdHgTe with x=0.30 for the material with *n*– (*1,4*) and *p*–type (*2,3*) conductivity.

Contributions from a number of effects, which are specific to the studied nanostructures, were initially considered for the explanation of the phenomenon of their intensive emission at high temperatures [16]. The effects included: *i*) localization of electrons, which were excited by Auger recombination, within the well (as opposed to the case of bulk material, where excited electrons move away and cannot participate in radiative recombination; *ii*) production of extra electron–hole pairs as a result of the impact ionization that takes place near the hetero–interface in structures with deep potential wells; and *iii*) localization of excitons/carriers at compositional disorder in the alloy. Careful examination of the experimental data, however, allowed for excluding the effect (*ii*) from consideration, as about 50 % of the nanostructures studied did not possess potential barriers high enough to provide impact ionization. On the other hand, recent modeling of recombination processes in solid solutions with large-scale compositional fluctuations showed that intensive luminescence from such solid solutions is indeed possible as a result of substantial increase of carrier concentration in fluctuation-induced potential minima of the energy gap [17]. This model also allows the emission spectrum to contain several bands due to radiative recombination in the local areas with the composition other than that in the basic matrix of the alloy. While the results of the modeling are yet to be brought to the final agreement with the experimental data, the effect of high–temperature photoluminescence of CdHgTe–based nanostructures clearly shows good prospects for manufacturing high–temperature infrared light emitters.

3.3. Photoluminescence of quantum-well structures. Photoluminescence of CdHgTe–based QWs has been discussed in our earlier works [18,19]. Structures with d_w=12 and 33 nm were studied, with optical transitions expected to occur between quantization levels. Our study allowed us to claim observation of such transitions as *c1–hh1*, *c1–hl1, c2–hh2*, where *c*

relates to quantization levels of electrons, *hh* relates to levels of heavy holes, and *hl* relates to levels of light holes. It should be noted that the observation of radiative transitions between quantization levels of electrons and light holes is favored in such structures due to the fact that wave functions of the electron and light hole states are mixed up, as is predicted by Kane's model [20], which describes CdHgTe structures best. This makes CdHgTe–based nanostructures with QWs an interesting object of optical studies.

3.4. Effect of annealing and spacer layer doping. It has been already shown that annealing improves the PL properties of MBE–grown CdHgTe films. This effect at low temperatures is generally expressed in narrowing of the FWHM of the excitonic lines, reduction of the Stokes shift and increase of the PL intensity [11,12]. A similar effect was observed for the studied nanostructures, including high–temperature PL spectra. The PL intensity at 84 K increased almost fivefold in structures #10 and #11 after the treatment, and at 300 K, the intensity increased in about 1.5 to 2 times. Also, in the annealed structures, the FWHM of the PL lines at 84 K decreased by 10 to 25 %, and at 300 K, the FWHM decreased by 10 to 15 %. For structure #10, after annealing the spectrum at 84 K comprised only one line, which showed that the acceptor levels observed in the as-grown structure were not related to an impurity, but rather to a structural defect. These results indicate that annealing indeed improves the ordering in MBE–grown CdHgTe.

Regarding the spacer layer doping, at 84 K structure #11 showed PL intensity approximately 3 times stronger than that of structure #10, where spacers were not doped. (Considering different value of E_g in the wells (and different non–radiative recombination rates, correspondingly), the actual increase might be smaller than that). At 300 K, we observed increase in the PL intensity of the order of few percent. This could be related to the effect of doping, which introduced additional carriers.

4. Conclusion

In conclusion, light emission from CdHgTe nanostructures was studied. The structures were grown by molecular beam epitaxy on GaAs substrates. For most of the structures with broad potential wells, the low–temperature PL spectra contained a single Gaussian–shape line, but closer to room temperature, a considerable broadening and distortion of the shape of the spectra was observed. The annealing of the nanostructures led to significant increase in the photoluminescence intensity and decrease in the spectral line width. One of the interesting effects observed during the study was a small decrease in the PL intensity with temperature increasing from 84 to 300 K. The possible reason for this effect is the localization of carriers at potential fluctuations induced by the technology–related alloy disorder. For quantum-well structures, optical transitions between the quantization levels for electrons and light holes were observed, which is believed to be favored by the fact of intermixing of wave functions of the electron and light hole states. The results of the study showed good prospects for CdHgTe nanostructures as the basis for optically-pumped infrared light emitters, including those operating at high (up to 300 K) temperatures.

Acknowledgement

The authors acknowledge the support of International Research Laboratory Program at ITMO University.

References

[1] C.R. Tonheim, A.S. Sudbø, E. Selvig, R. Haakenaasen // *IEEE Photonics Technology Letters* **23** (2011) 36.

[2] J.P. Zanatta, F. Noël, P. Ballet, N. Hdadach, A. Million, G. Destefanis, E. Mottin, C. Kopp, E. Picard, E. Hadji // *Journal of Electronic Materials* **32** (2003) 602.

[3] R.D. Feldman, C.L. Cesar, M.N. Islam, R.F. Austin, A.E. DiGiovanni, J. Shah, R. Spitzer, J. Orenstein // *Journal of Vacuum Science and Technology B* **7** (1989) 431.
[4] K.K. Mahavadi, M.D. Lange, J.P. Faurie, J. Nagle // *Applied Physics Letters* **54** (1989) 2580.
[5] E. Monterrat, L. Ulmer, R. Mallard, N. Magnea, J.L. Pautrat, H. Mariette // *Journal of Applied Physics* **71** (1992) 1774.
[6] E. Hadji, J. Bleuse, N. Magnea, J.L. Pautrat // *Applied Physics Letters* **67** (1995) 2591.
[7] E. Hadji, E. Picard, C. Roux, E. Molva, P. Ferret // *Optics Letters* **25** (2000) 725.
[8] M. Kinch // *Journal of Electronic Materials* **39** (2010) 1043.
[9] N.N. Mikhailov, R.N. Smirnov, S.A. Dvoretsky, Yu.G. Sidorov, V.A. Shvets, E.V. Spesivtsev, S.V. Rykhlitski // *International Journal of Nanotechnology* **3** (2006) 126.
[10] J.P. Laurenti, J. Camassel, A. Bouhemadou, B. Toulouse, R. Legros, A. Lusson // *Journal of Applied Physics* **67** (1990) 6454.
[11] K.D. Mynbaev, N.L. Bazhenov, V.I. Ivanov-Omskii, N.N. Mikhailov, M.V. Yakushev, A.V. Sorochkin, S.A. Dvoretsky, V.S. Varavin, Yu.G. Sidorov // *Semiconductors* **45** (2011) 872.
[12] V.I. Ivanov-Omskii, N.L. Bazhenov, K.D. Mynbaev // *Physica Status Solidi B* **246** (2009) 1858.
[13] A. Lusson, F. Fuchs, Y. Marfaing // *Journal of Crystal Growth* **101** (1990) 673.
[14] I.I. Izhnin, A.I. Izhnin, H.V. Savytskyy, O.I. Fitsych, N.N. MIkhailov, V.S. Varavin, S.A. Dvoretsky, Yu.G. Sidorov, K.D. Mynbaev // *Opto–Electronics Review* **20** (2012) 375.
[15] V.N. Abakumov, V.I. Perel, I.N. Yassievich, *Nonradiative Recombination in Semiconductors*, vol. 33 of *Modern Problems in Condensed Matter Science,* ed. by V.M. Agranovich and A.A. Maradudin (North-Holland, Amsterdam, 1991).
[16] A.I. Izhnin, A.I. Izhnin, K.D. Mynbaev, N.L. Bazhenov, A.V. Shilyaev, N.N. Mikhailov, V.S. Varavin, S.A. Dvoretsky, O.I. Fitsych, A.V. Voitsekhovsky // *Opto-Electronics Review* **21** (2013) 390.
[17] A.V. Shilyaev, A.A. Greshnov, N.L. Bazhenov, K.D. Mynbaev // *Materials Physics and Mechanics* **18(2)** (2013) 171.
[18] N.L. Bazhenov, A.V. Shilyaev, K.D. Mynbaev, G.G. Zegrya // *Semiconductors* **46**, (2012) 773.
[19] A.V. Voitsekhovskii, D.I. Gorn, I.I. Izhnin, A.I. Izhnin, V.D. Goldin, N.N. Mikhailov, S.A. Dvoretskii, Yu.G. Sidorov, M.V. Yakushev, V.S. Varavin // *Russian Physics Journal* **55** (2013) 910.
[20] A.P. Polkovnikov, G.G. Zegrya // *Physical Review B* **58** (1998) 4039.